



AFRL-RX-TY-TR-2009-4566

THE ATOMIC FORCE MICROSCOPIC (AFM) CHARACTERIZATION OF NANOMATERIALS

LaTashia Burgans

Prairie View A&M University
College of Engineering
Prairie View, TX 77446-0519

Contract No. FA4819-07-D-0001

JUNE 2009

DISTRIBUTION A: Approved for public release; distribution unlimited.

**AIR FORCE RESEARCH LABORATORY
MATERIALS AND MANUFACTURING DIRECTORATE**

■ Air Force Materiel Command ■ United States Air Force ■ Tyndall Air Force Base, FL 32403-5323

DISCLAIMER

Reference herein to any specific commercial product, process, or service by trade name, trademark, manufacturer, or otherwise does not constitute or imply its endorsement, recommendation, or approval by the United States Air Force. The views and opinions of authors expressed herein do not necessarily state or reflect those of the United States Air Force.

This report was prepared as an account of work sponsored by the United States Air Force. Neither the United States Air Force, nor any of its employees, makes any warranty, expressed or implied, or assumes any legal liability or responsibility for the accuracy, completeness, or usefulness of any information, apparatus, product, or process disclosed, or represents that its use would not infringe privately owned rights.

NOTICE AND SIGNATURE PAGE

Using Government drawings, specifications, or other data included in this document for any purpose other than Government procurement does not in any way obligate the U.S. Government. The fact that the Government formulated or supplied the drawings, specifications, or other data does not license the holder or any other person or corporation; or convey any rights or permission to manufacture, use, or sell any patented invention that may relate to them.

This report was cleared for public release by the Air Force Research Laboratory Airbase Technologies Division Public Affairs Office and is available to the general public, including foreign nationals. Copies may be obtained from the Defense Technical Information Center (DTIC) (<http://www.dtic.mil>).

AFRL-RX-TY-TR-2009-4566 HAS BEEN REVIEWED AND IS APPROVED FOR PUBLICATION IN ACCORDANCE WITH ASSIGNED DISTRIBUTION STATEMENT.

//signature//
PAUL E. SHEPPARD
Work Unit Manager

//signature//
SANDRA R. MEEKER, DR-IV
Chief, Airbase Engineering Development Branch

//signature//
ALBERT N. RHODES, PhD
Chief, Airbase Technologies Division

This report is published in the interest of scientific and technical information exchange, and its publication does not constitute the Government's approval or disapproval of its ideas or findings.

REPORT DOCUMENTATION PAGE

*Form Approved
OMB No. 0704-0188*

The public reporting burden for this collection of information is estimated to average 1 hour per response, including the time for reviewing instructions, searching existing data sources, gathering and maintaining the data needed, and completing and reviewing the collection of information. Send comments regarding this burden estimate or any other aspect of this collection of information, including suggestions for reducing the burden, to Department of Defense, Washington Headquarters Services, Directorate for Information Operations and Reports (0704-0188), 1215 Jefferson Davis Highway, Suite 1204, Arlington, VA 22202-4302. Respondents should be aware that notwithstanding any other provision of law, no person shall be subject to any penalty for failing to comply with a collection of information if it does not display a currently valid OMB control number.

PLEASE DO NOT RETURN YOUR FORM TO THE ABOVE ADDRESS.

1. REPORT DATE (DD-MM-YYYY) 30-JUN-2009	2. REPORT TYPE Final Technical Report	3. DATES COVERED (From - To) 02-SEP-2008 -- 30-JUN-2009
---	---	---

4. TITLE AND SUBTITLE The Atomic Force Microscopic (AFM) Characterization of Nanomaterials	5a. CONTRACT NUMBER FA4819-07-D-0001
	5b. GRANT NUMBER
	5c. PROGRAM ELEMENT NUMBER 62102F

6. AUTHOR(S) Burgans, LaTashia	5d. PROJECT NUMBER 4915
	5e. TASK NUMBER F2
	5f. WORK UNIT NUMBER Q210FA72

7. PERFORMING ORGANIZATION NAME(S) AND ADDRESS(ES) Prairie View A&M University College of Engineering Prairie View, TX 77446-0519	8. PERFORMING ORGANIZATION REPORT NUMBER
---	---

9. SPONSORING/MONITORING AGENCY NAME(S) AND ADDRESS(ES) Air Force Research Laboratory Materials and Manufacturing Directorate Airbase Technologies Division 139 Barnes Drive, Suite 2 Tyndall Air Force Base, FL 32403-5323	10. SPONSOR/MONITOR'S ACRONYM(S) AFRL/RXQEM
	11. SPONSOR/MONITOR'S REPORT NUMBER(S) AFRL-RX-TY-TR-2009-4566

12. DISTRIBUTION/AVAILABILITY STATEMENT
Distribution Statement A: Approved for public release; distribution unlimited.

13. SUPPLEMENTARY NOTES
Ref AFRL/RXQ Public Affairs Case # 10-128. Document contains color images.

14. ABSTRACT
This research utilized atomic force microscopy (AFM) in the characterization of nanomaterials. The research also discussed the characterization observations pertaining to the dispersion of nanomaterials used in the study. The examination results showed that the dispersed nanomaterials could be divided into partially dispersed and fully dispersed states which were clearly distinguishable from the images obtained via AFM. Material characterization was initially made using optical microscopy (OM) and then with atomic force microscopy (AFM).
In this research, we attempted to determine the best dispersion method that would easily disperse the carbon nanotubes. The carbon nanotubes are immersed in the solvent *N,N*-dimethylformamide (DMF). In recent studies DMF has been reported as a good solvent for the dispersion of nanotubes. And during our experiments, only DMF provided the desired "fully dispersed state". A tip sonicator was used during the dispersion method.
We determined that the carbon nanotube (CNTs) dispersion level could be roughly indentified from the OM images. In this work, the relationship between OM images and those obtained from AFM images was examined. The examination results showed that the nanomaterials could be divided into partially dispersed and fully dispersed states, which were clearly viewed from the AFM images.

15. SUBJECT TERMS
nanotube, CNT, dispersion, DMF, sonicator, characterization

16. SECURITY CLASSIFICATION OF:			17. LIMITATION OF ABSTRACT UU	18. NUMBER OF PAGES 31	19a. NAME OF RESPONSIBLE PERSON Paul E. Sheppard
a. REPORT U	b. ABSTRACT U	c. THIS PAGE U			19b. TELEPHONE NUMBER (Include area code)

Reset

TABLE OF CONTENTS

1.0 INTRODUCTION	1
1.1 Carbon Nanotubes	1
1.2 Atomic Force Microscope (AFM).....	4
1.3 Optical Microscope (OM).....	7
2.0 LITERATURE REVIEW	8
2.1 Dispersion of Carbon Nanotubes	8
2.2 Sorting of Dispersion Carbon Nanotubes.....	9
3.0 EXPERIMENTAL	10
3.1 Dispersion of Nanomaterials.....	11
4.0 RESULTS AND DISCUSSION	12
4.1 Dispersion of SWNTs	12
4.2 Ball Milling and Dispersion of XD Nanotubes (XCDNTs) and Tungsten Carbide (WC) ..	13
5.0 CONCLUSIONS	18
6.0 REFERENCES	19
7.0 LIST OF SYMBOLS, ABBREVIATIONS AND ACRONYMS	22

LIST OF FIGURES

1	3D Model of Three Types of Single-Walled Carbon Nanotubes	2
2	Surface Image of Double-Walled Carbon Nanotube Bundles.....	3
3	Block Diagram of Atomic Force Microscope	5
4	Schematic of How AFM Works	5
5	View of Cantilever in Atomic Force Microscope, Magnification 1000x	6
6	AFM (Used) Cantilever in Scanning Electron Microscope, Magnification 3000x	6
7	Several Types of Microscopes.....	7
8	OM on Mica Surface	12
9	AFM on Mica Surface	12
10	OM Images SWNTs on Mica After 1) 30 Minutes, b) 60 Minutes, c) 90 Minutes, d) 120 Minutes, Respectively.....	13
11	AFM Image of XDCNTs/WC After Ball Milling for 20 Minutes (Scan Size 10 μm).....	14
12	AFM Image of XDCNTs/WC After Ball Milling for 20 Minutes (Scan size 2 μm)	14
13	AFM Image of XDCNTs/WC After Ball Milling for 40 Minutes (Scan Size 10 μm).....	15
14	AFM Image and Section Analysis of XDCNTs/WC After Ball Milling for 40 Minutes (Scan Size 2 μm).....	15
15	AFM Image of XDCNTs/WC After Ball Milling for 100 Minutes (Scan size 10 μm)	16
16	AFM Image and Length Measurement of XDCNTs/WC After Ball Milling for 100 Minutes	16
17	AFM Image of XDCNTs/WC After Ball Milling for 160 Minutes.....	17

LIST OF TABLES

1	Comparison of Mechanical Properties of CNTs and Other Materials.....	4
2	Tapping Mode Tip Specifications	10

ABSTRACT

This research primarily utilized atomic force microscopy (AFM) in the characterization of nanomaterials. The research also discussed the characterization observations pertaining to the dispersion of nanomaterials used in the study. The examination results showed that the dispersed nanomaterials could be divided into partially dispersed and fully dispersed states, which were clearly distinguishable in the images obtained via AFM. Material characterization was initially made using optical microscopy (OM) and then with AFM.

Carbon nanotubes (CNT) comprising both single-walled nanotubes (SWNTs) and multi-walled nanotubes (MWNTs) were characterized via AFM. Electrical grade (XD) Nanotubes, another mixture that was characterized via AFM, consisted of either SWNTs or both SWNTs and MWNTs. During characterization, the SWNTs range from 1 to 1.5 nm in diameter, and the MWNTs range from 5 to 30 μm in diameter.

In this research, we attempted to determine the best dispersion method that would easily disperse the carbon nanotubes. The carbon nanotubes are immersed in the solvent *N,N*-dimethylformamide (DMF). In recent studies DMF has been reported as a good solvent for the dispersion of nanotubes. And during our experiments, only DMF provided the desired “fully dispersed state”. A tip sonicator was used during the dispersion method.

Under high magnification, OM was used to observe nanomaterial dispersion throughout the surface area. The quick overview using OM aided in the acquisition of quality AFM images. The chances of obtaining quality images from the AFM were further enhanced if a decent amount of dispersed nanomaterial was viewed under the optical microscope.

An important reason for using the AFM in characterization studies is the fact that there are few restrictions prior to or after the analysis of a sample. The AFM data contain important information which was determined throughout the structural analysis of the surface. And during this AFM characterization process, the tapping mode and tip were utilized. While viewing the images from the AFM, we critiqued three primary image parameters: the surface height, amplitude, and phase. Each AFM image parameter described a different topographical view from the surface. The height image is the image from the scanner. The amplitude images are from the photo detector inside the microscope. The phase image detects the change in the sine curve. Therefore, when characterizing the best images from the surface, we use either two out of the three image parameters, or all of them.

We determined that the CNTs' dispersion level could be roughly indentified from the OM images. In this work, the relationship between OM images and those obtained from AFM images was examined. The examination results showed that the nanomaterials could be divided into partially dispersed and fully dispersed states, which were clearly visible in the AFM images. And in this research, DMF was utilized as the solvent to provide a fully dispersed state.

ACKNOWLEDGEMENTS

The author of this report would like to acknowledge the funding received from the Air Force Research Laboratory, Airbase Technologies Division (AFRL/RXQ) at Tyndall Air Force Base (AFB), Florida through the Supplemental Support Group (SSG) program. All through the program, Mr. Ian Welch, Applied Research Associates contractor at Tyndall AFB, supported my efforts. His encouragement was a driving force for the completion of this research, and I, Latashia Burgans, sincerely appreciate his efforts on my behalf.

1. INTRODUCTION

Since the discovery of CNTs by Iijima [1], extensive studies have been conducted exploring their unique electronic, thermal, optical, and mechanical properties, and their potential use in greatly enhancing the physical properties of polymer nanocomposites [2-6]. As summarized in recent review articles [7,8], the outstanding properties of polymer nanocomposites are, in part, attributed to their extremely high aspect ratio of up to 1000. It is often stated that the full realization of the reinforcement potential of CNTs requires good spatial dispersion of the carbon nanotube [7]. To address this problem we must initially determine some objective method for defining what “good dispersion” means. In particular, we need some kind of dispersion method to evaluate the role of dispersion in the nanomaterials.

The following methods have been used to achieve well-dispersed CNTs in a polymer: functionalization of the CNT walls [9,10], the use of surfactants [11], the controlled duration of sonication of mixtures of CNTs in various solvents [12-16], in situ polymerization under sonication [17], in situ bulk polymerization [18], high speed mechanical stirring [19,20], and compounding using a twin-screw extruder [21,22]. The dispersion method of nanomaterials in DMF was primarily determined from images acquired using AFM and OM. Most studies undertaken, however, provided only a qualitative measure of dispersion of the CNTs without a specification of the length of the scale over which these characterizations were made, along with the scale over which these metrics were applied. A quantitative measure for the spatial dispersion of nanoparticles was critically needed to understand the relationship between the original sample characterization and the physical properties of the nanocomposites [23]. Further improvements in the physical properties of the nanocomposite could also be achieved from such a relationship [24].

1.1 Carbon Nanotubes

CNTs are allotropes of carbon with a cylindrical nanostructure that can have a length-to-diameter ratio of up to 28,000,000:1 [25], which is significantly larger than any other material. The carbon nanotube molecules have novel properties that make them potentially useful in many applications within the fields of nanotechnology, electronics, optics, and other material science disciplines, including architecture. CNTs exhibit extraordinary strength and unique electrical properties and are efficient conductors of heat. Their final usage, however, may be limited by their potential toxicity to humans.

Nanotubes are members of the fullerene structural family, which also includes the spherical buckyballs (Fig. 1). The ends of a nanotube might be capped with a hemisphere of the buckyball structure. Their name is derived from their size; while the diameter of a nanotube is on the order of a few nanometers (approximately 1/50,000th of the width of a human hair), their length (as of 2008) can be up to several millimeters. Nanotubes are categorized as SWNTs and MWNTs.

The nature of bonding within a nanotube is described by applied quantum chemistry, specifically, orbital hybridization. The chemical bonding of nanotubes is composed entirely of sp^2 bonds, similar to those of graphite. This bonding structure, which is stronger than the sp^3 bonds found in diamonds, provides the molecules with their unique strength. Nanotubes

naturally align themselves into "ropes" held together by Van der Waals forces. Under high pressure, nanotubes can merge together via sp^2 bond exchange for sp^3 bonds, giving the possibility of producing strong, infinite-length wires through high-pressure nanotube linking.

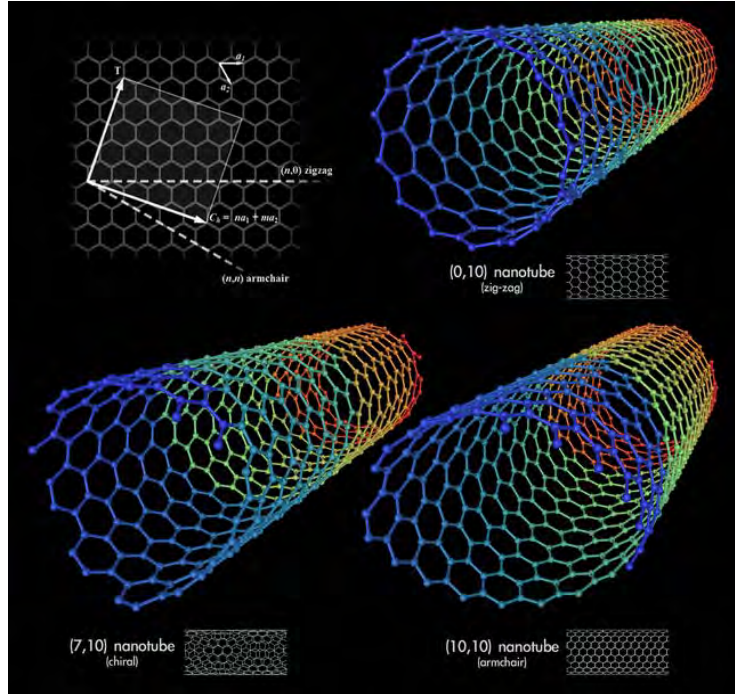


Figure 1. 3D Model of Three Types of Single-Walled Carbon Nanotubes

Most SWNTs have a diameter of close to 1 nm, and a tube length that can be millions of times longer. The structure of a SWNT can be conceptualized by wrapping a one-atom-thick layer of graphite, called graphene, into a seamless cylinder. The way the graphene sheet is wrapped is represented by a pair of indices (n, m) called the chiral vector. The integers n and m denote the number of unit vectors along two directions in the honeycomb crystal lattice of graphene. If $m=0$, the nanotubes are called "zigzag". If $n=m$, the nanotubes are called "armchair". Otherwise, they are "chiral".

Single-walled nanotubes are an important variety of carbon because they exhibit electric properties that are not shared by the MWNT variants. Single-walled nanotubes are the most likely candidate for miniaturizing electronics beyond the micro electromechanical scale currently used in electronics. The most basic building block of these systems is the electric wire, and SWNTs can be excellent conductors.[26][27] One useful application of SWNTs is in the development of the first intramolecular field effect transistors (FETs). Additionally, the first intramolecular logic gate utilizing SWNT FETs has recently become possible as well.[28] To create a logic gate, you must have both a p -FET and an n -FET. Because SWNTs are p -FETs when exposed to oxygen and n -FETs otherwise, it is possible to protect half of an SWNT from oxygen exposure, while exposing the other half to oxygen. This results in a single SWNT acting as a NOT logic gate, with both p and n -type FETs within the same molecule.

Single-walled nanotubes are still very expensive to produce, around \$1500 per gram as of the year 2000, and the development of more affordable synthesis techniques is vital to the future of carbon nanotechnology. If a cheaper means of synthesis cannot be discovered, it would be financially impossible to apply this technology towards commercial-scale applications.[29] Fortunately, as of 2007 several suppliers offer as-produced arc discharge SWNTs for ~\$50 to \$100 per gram.[30][31]

MWNTs consist of multiple rolled layers (concentric tubes) of graphite. There are two models which can be used to describe the structures of multi-walled nanotubes. In the Russian doll model, sheets of graphite are arranged in concentric cylinders, e.g., a (0,8) SWNT within a larger (0,10) SWNT. In the Parchment model, a single sheet of graphite is rolled in around itself, resembling a scroll of parchment or a rolled newspaper. The interlayer distance in multi-walled nanotubes is close to the distance between graphene layers in graphite, approximately 3.3 Å (330 pm). Double-walled carbon nanotubes (DWNTs) shown in Figure 2, must be included in this discussion because their morphology and properties are similar to those viewed in SWNTs; however, DWNTs are far more resistant to chemicals than are SWNTs. This is especially important when functionalization, the grafting of chemical functions at the surface of the nanotubes, is required to add new properties to the CNT. In the case of SWNTs, covalent functionalization will break some of the C=C double bonds, leaving "holes" in the structure of the nanotube, and modifying both its mechanical and electrical properties. In the case of DWNTs, only the outer wall is modified. DWNT synthesis on the gram scale was first proposed in 2003[32] by the Combustion Chemical Vapor Deposition (CCVD) technique, the selective reduction of oxide solutions in methane and hydrogen.



Figure 2. Surface Image of Double-Walled Carbon Nanotube Bundles

Now in terms of tensile strength and elastic modulus, carbon nanotubes are among the strongest and most rigid materials yet discovered. This strength results from the covalent sp^2 bonds formed between the individual carbon atoms. In 2000, a multi-walled carbon nanotube (MWCT) was tested to have a tensile strength of 63 gigapascals (GPa), which translates into the CNT's ability to endure the weight of 6300 kg on a cable with a cross-section of 1 mm². And since carbon nanotubes have a low density for a solid, about 1.3-1.4 g·cm⁻³ [30], its specific

strength of up to $48,000 \text{ kN}\cdot\text{m}\cdot\text{kg}^{-1}$ is the highest among known materials, as compared to high-carbon steel's strength of $154 \text{ kN}\cdot\text{m}\cdot\text{kg}^{-1}$.

Under excessive tensile strain the nanotubes will undergo plastic deformation, meaning that the deformation transformation is permanent. The deformation begins at strains of approximately 5%; however, by releasing the strain energy, CNTs can increase their maximum strain before fracturing can occur.

CNTs (Table 1) are not nearly as strong under compression. Because of their hollow structure and high aspect ratio, they tend to buckle when placed under compressive, torsional or bending stress.

Table 1. Comparison of Mechanical Properties of CNTs and Other Materials [32]

Comparison of Mechanical Properties			
Material	Young's Modulus (TPa)	Tensile Strength (GPa)	Elongation at Break (%)
SWCNT	~1 (from 1 to 5)	13-53 ^E	16
Armchair SWCNT	0.94 ^T	126.2 ^T	23.1
Zigzag SWCNT	0.94 ^T	94.5 ^T	15.6-17.5
Chiral SWCNT	0.92		
MWCNT	0.8-0.9 ^E	150	
Stainless Steel	~0.2	~0.65-1	15-50
Kevlar	~0.15	~3.5	~2
Kevlar ^T	0.25	29.6	

^EExperimental observation ; ^TTheoretical prediction

The aforementioned discussion referred to axial properties of the nanotube, whereas simple geometrical considerations suggest that carbon nanotubes should be much softer in the radial direction, than along the tube axis. Indeed, transmission electron microscopic (TEM), observation of radial elasticity suggested that even van der Waals forces can deform two adjacent nanotubes[33]. Nanoindentation experiments, performed by several groups on MWNTs [34][35], indicated a Young's modulus in the order of several GPa, confirming that CNTs are indeed rather soft in the radial direction.

1.2 Atomic Force Microscope (AFM)

The AFM, or scanning force microscope (SFM), is a very high-resolution type of scanning probe microscope, with demonstrated resolution of a fraction of a nanometer, more than 1000 times higher than the optical diffraction limit. The precursor to the AFM, the scanning tunneling microscope, was developed by Gerd Binnig and Heinrich Rohrer in the early 1980s, a development that earned them the Nobel Prize for Physics in 1986. Binnig, Quate and Gerber

invented the first AFM in 1986. The AFM is one of the foremost tools for imaging, measuring, and manipulating matter at the nanoscale (Figures 3 and 4). The information is gathered by "feeling" the surface with a microscale cantilever, a sharp tip (probe) at its end that is used to scan the specimen surface. The cantilever is typically silicon or silicon nitride with a tip radius on the order of several nanometers. Piezoelectric elements that facilitate tiny, but accurate and precise movement on the electronic command enable the AFM to have very precise scanning.

When the tip is brought into proximity of a sample surface, forces between the tip and the sample lead to a deflection of the cantilever according to Hooke's law. Depending upon the situation, forces that are measured by AFM include mechanical contact force, Van der Waals forces, capillary forces, chemical bonding, electrostatic forces, magnetic forces (see magnetic force microscope (MFM)), Casimir forces, solvation forces, etc. In addition to these forces, other quantities could also be simultaneously measured through the use of a specialized type of probe (see Scanning thermal microscopy, photothermal microspectroscopy, etc.). Typically, the deflection is measured using a laser spot reflected from the top surface of the cantilever into an array of photodiodes. Other methods that are used include optical interferometry, capacitive sensing, or piezoresistive AFM cantilevers. These cantilevers are fabricated with piezoresistive elements that act as a strain gauge. Using a Wheatstone bridge, strain in the AFM cantilever due to deflection can be measured, but this method is not as sensitive as laser deflection or interferometry.

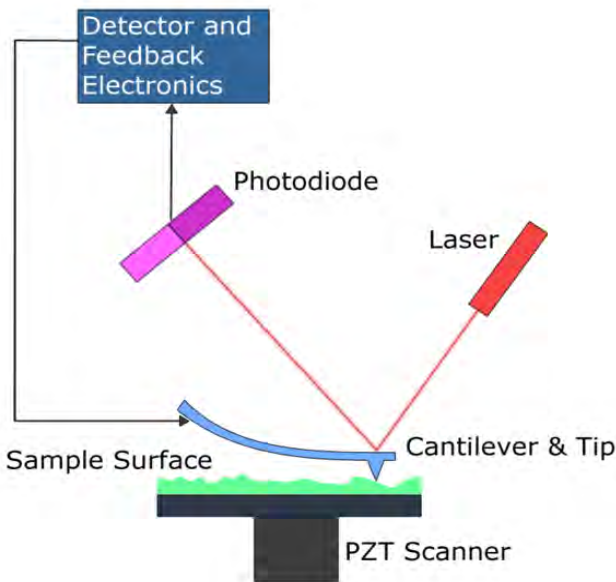


Figure 3. Block Diagram of Atomic Force Microscope

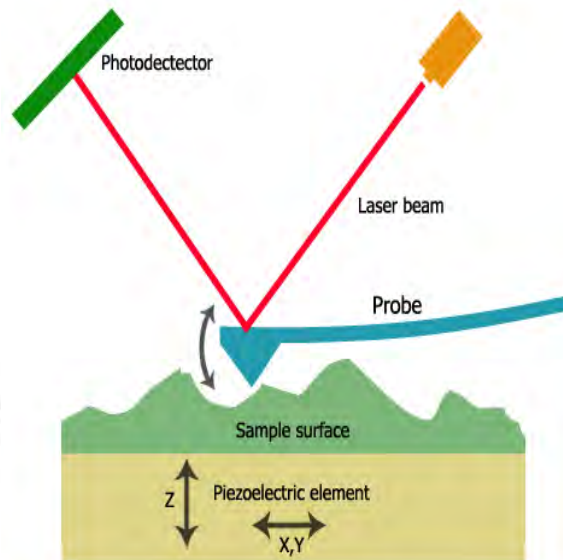


Figure 4. Schematic of How AFM Works

If the tip was scanned at a constant height, a risk exists due to the possibility of the tip being damaged upon collision with the surface. Hence, in most cases a feedback mechanism is employed to adjust the tip-to-sample distance, and to maintain a constant force between the tip and the sample. Traditionally, the sample is mounted on a piezoelectric tube that can move the sample in the z direction for maintaining a constant force, and the x and y directions for scanning

the sample. Alternatively, a “tripod” configuration of three piezo crystals may be employed, with each responsible for scanning in the x , y and z directions. This eliminates some of the distortion effects seen with a tube scanner. In newer designs, the tip is mounted on a vertical piezo scanner while the sample is being scanned in x and y using another piezo block. The resulting map of the area $s = f(x,y)$ represents the topography of the sample.

The AFM can be operated in a number of modes, depending on the application. In general, the possible imaging modes are divided into static (also called contact) modes and a variety of dynamic (or non-contact) modes where the cantilever is vibrated.

In tapping mode, the cantilever is driven to oscillate up and down at near its resonance frequency by a small piezoelectric element mounted in the AFM tip holder (Figure 5 and 6). The amplitude of this oscillation is greater than 10 nm, typically 100 to 200 nm. Due to the interaction of forces acting on the cantilever, when the tip approaches the surface, forces including Van der Waals, electrostatic, or dipole-dipole interactions cause the amplitude of this oscillation to decrease as the tip gets closer to the sample. An electronic servo uses the piezoelectric actuator to control the height of the cantilever above the sample. The servo adjusts the height to maintain a set cantilever oscillation amplitude as the cantilever is scanned over the sample. A Tapping AFM image is, therefore, produced by imaging the force of the oscillating contacts of the tip with the sample surface. This is an improvement on conventional contact AFM, in which the cantilever just drags across the surface at constant force and can result in surface damage. The tapping mode is gentle enough even for the visualization of supported lipid bilayers, or adsorbed single polymer molecules (for instance, 0.4 nm thick chains of synthetic polyelectrolytes) under liquid medium. At the application of proper scanning parameters, the conformation of single molecules remains unchanged for hours (Roiter and Minko, 2005).

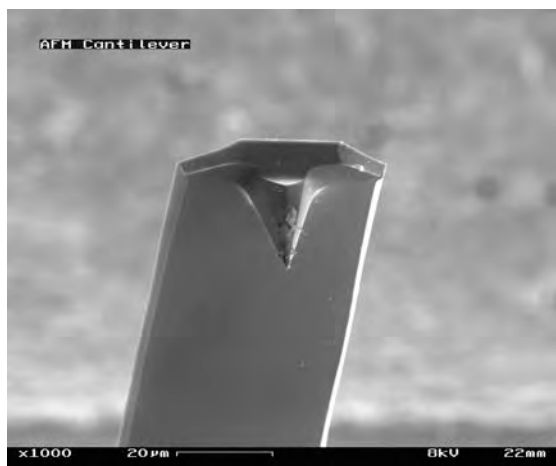


Figure 5. AFM Cantilever (After Use) in the Scanning Electron Microscope Magnification 1,000 x (Image Width ~ 100 Micrometers)

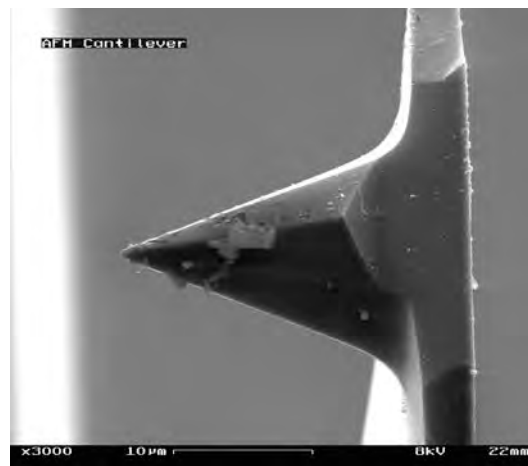


Figure 6. AFM Cantilever (After Use) in the Scanning Electron Microscope, Magnification 3,000 x (Image Width ~ 30 Micrometers)

1.3 Optical Microscope

Optical microscopes (OMs), through their use of visible wavelengths of light, are the simplest and hence most widely used type of microscope (Figure 7). OMs typically use refractive glass, and occasionally plastic or quartz, to focus light into the eye or another light detector. Mirror-based optical microscopes operate in the same manner. Typical magnification of a light microscope, assuming visible range light, is up to 1500x with a theoretical resolution limit of around 0.2 μm or 200 nm. Specialized techniques (e.g., scanning confocal microscopy, Vertico SMI) may exceed this magnification but the resolution is diffraction limited. Using shorter wavelengths of light, such as the ultraviolet, is one way to improve the spatial resolution of the microscope, as are techniques such as the Near-field scanning optical microscope.

Various wavelengths of light, including those beyond the visible range, are sometimes used for special purposes. Ultraviolet light is used to enable the resolution of smaller features as well as to image samples that are transparent to the eye. Near infrared light is used to image circuitry embedded in bonded silicon devices as silicon is transparent in this region. Many wavelengths of light, ranging from the ultraviolet to the visible are used to excite fluorescence emission from objects for viewing by eye or with sensitive cameras.

Phase contrast microscopy is an optical microscopy illumination technique in which small phase shifts in the light passing through a transparent specimen are converted into amplitude or contrast changes in the image. A phase contrast microscope does not require staining to view the slide. This microscope made it possible to study the cell cycle.

The digital microscope appeared a few years ago, using optics and a charge-coupled-device (CCD) camera to output a digital image to a monitor.

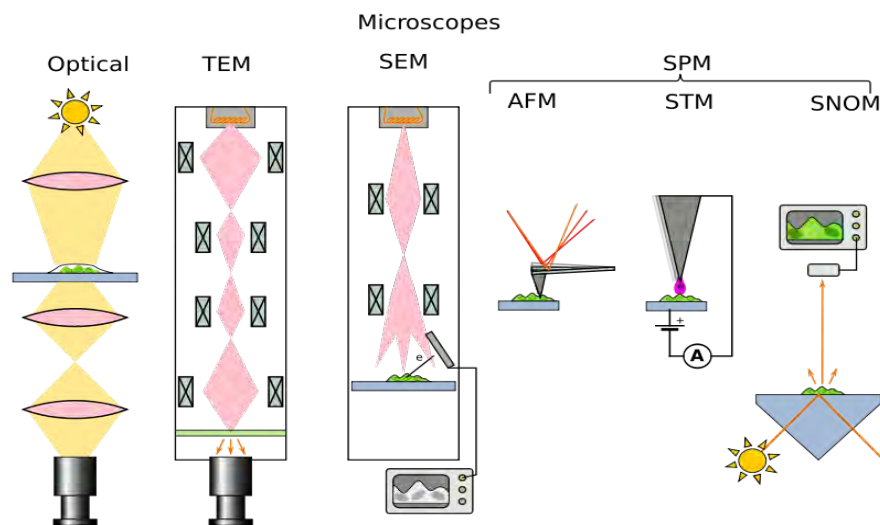


Figure 7. Several Types of Microscopes

Three major variants of electron microscopes exist:

Scanning electron microscope (SEM): views the surface of bulk objects by scanning the surface with a fine electron beam and measuring its reflection. It may also be used for spectroscopy.

TEM: passes electrons completely through the sample, analogous to basic optical microscopy. This requires careful sample preparation, since electrons are scattered so strongly by most materials. This is a scientific device that allows people to see objects that could normally not be seen by the naked or unaided eye.

Scanning tunneling microscope (STM): a powerful technique for viewing surfaces at the atomic level.

The SEM and STM are also considered examples of scanning probe microscopy.

2. LITERATURE REVIEW

In this study CNTs were dispersed in different solvents including DMF, cosolvent isopropyl alcohol (IPA)/water, and trichloroethane (TCA), using a bath sonication technique. The following review includes the sorting of CNTs in solutions that could be used for CNTs dispersion.

2.1 Dispersion of Carbon Nanotubes

In 1999, Jie Liu et al.[41] reported that amide solvents, such as DMF and *N*-methylpyrrolidone (NMP), are good solvents for SWNTs dispersion. In his report, SWNTs were prepared with the pulsed laser vaporization (laser ablation) method and purified by HNO₃. The solution of SWNTs/DMF was prepared at a concentration of 0.1 mg/mL and bath sonicated for 15 hours. The resulting individual SWNTs dispersed on mica were characterized by AFM. The solution was also stable at room temperature and could be stored for several months without precipitation. The author also reported that SWNTs in DMF suspensions specifically absorbed onto amino-functionalized (-NH₂) surfaces. Although this work reported the DMF dispersions to be stable suspensions, Kevin et al.[42] suggested that the dispersions aggregate on a time scale of days. Upon observing trends in solubilization and various solubility parameters, Kevin et al. also suggested that the optimum solvents for SWNT dispersion should have both high electron pair donicity (β) and low hydrogen bond parameter (α). Both NMP and DMF solvents met this criteria. Dimethyl sulfoxide (DMSO) also met these criteria; however, it showed only moderate results. Kevin et al. concluded that though the β and α parameters were important, additional conditions may need to be determined.

Later, Bumsu et al. [43] reported that α -terpineol and Texanol were better solvents than DMF due to their larger chemical structures and higher viscosity (α -terpineol 36.5 cP, Texanol 18.3 cP, DMF 0.802 cP). This high viscosity may enhance the dispersity of the SWNT suspensions by reducing the attractive forces between them. Furthermore, the mobility of the SWNTs may be reduced as well in α -terpineol or Texanol. The solutions were sonicated for 15 minutes with very mild conditions (300 W, 40 KHz, room temperature), and characterized by OM. In comparing the three solvents used, SWNTs/ α -terpineol showed better dispersity and longer stabilization.

2.2 Sorting of Dispersion of Carbon Nanotubes

The dispersion of nanotubes in solvents with agitation assist has proven to provide high dispersion levels. This form of dispersion can be used for CNTs in many applications. However, for applications in which electrical conductivities are crucial, dispersed nanotubes need to be sorted and categorized. Several methods have been developed to enhance the population purity of individual nanotube species, including electrophoresis, dielectrophoresis, and ion exchange chromatography, though the throughput is limited [49]. Arnold *et al.*[50] used density-gradient ultracentrifugation to sort the carbon nanotubes by diameter, band gap and electronic type. Several surfactants, including sodium dodecyl sulfate (SDS), sodium dodecylbenzenesulfonate (SDBS), sodium chlorate (SC), sodium deoxycholate and sodium taurodeoxycholate were used to encapsulate SWNTs. The SWNTs/surfactant solutions were put under relative centrifugal forces (RFC) of 174,000 to 207,000 *g* for 9 to 24 hours. The encapsulated SWNTs were forced into separate layers by their buoyancy differences. The author suggested that this might be caused by the surfactants' organization around SWNTs comprising different structures and electronic types. It was claimed that this technique was scalable and highly compatible with subsequent processing techniques. A sharp diameter was claimed to be achieved, where more than 97% of semiconducting SWNTs were within 0.2 Å of the mean diameter. Fagan *et al.*[48] used a similar technique to sort between SWNTs with different lengths. The author used iodixanol (5,5₀-[(2-hydroxy-1-3 propanediyl)-bis(acetylimino)]bis[N,N₀-bis(2,3dihydroxylpropyl-2,4,6-triiodo-1,3-benzenecarboxamide)]) to generate solutions of varying density. It was shown that longer SWNTs traveled a greater velocity in the direction opposite to the applied acceleration. The longest SWNTs reached the top of the liquid within 20 hours and created length fractionation from the top to the bottom.

3.0 EXPERIMENTAL

This experiment used nanomaterial prepared by Clarkson Aerospace for detailed analysis of the composite powders. The mixture of carbon nanotubes was dispersed using DMF. DMF was chosen because, in recent studies of carbon nanotubes, it was determined to be a good solution for the dispersement of nanotubes. Afterwards, the mixture of 0.2 mg/80 mL was placed under a tip sonicator for 30 minutes, 60 minutes, 90 minutes, and 2 hours. Next, each time was recorded and a sample drop was placed on the mica for drying. The drying took 24 hours for each. The samples were then placed on the OM and AFM for imaging and characterization. The OM images were taken first. The AFM images were taken next for examination and discussion. The imaging procedures were repeated for each nanomaterial sample.

Another high-purity SWNT nanomaterial was purchased from Helix Material Solutions Inc. with the following specifications: fabrication method, Chemical Vapor Deposition (CVD); external diameter, ~1.3 nm.; length, 0.5 to 40 μm ; purity, >90%; amorphous carbon, < 5%, ash, <2 wt%; and the specific surface area, 300 to 600 m^2/g . The catalyst was not specified.

AFM images were obtained with a MultiModeTM scanning probe microscope (SPM) (Digital Instrument – Veeco, model MMAFM-2), Nanoscope IIIa controller (model NS3A) system with scanner type “E.” E scanners have a typical scan size of 10x10 μm and a vertical range of 2.5 μm . In most cases, the images were obtained with the tapping mode except where the surface topology varied abruptly; if it varies, the contact mode would be used. AFM tapping mode probes were obtained from Ted Pella Inc. The probes were made of silicon with the characteristics shown in Table 2, and were either coated with or without aluminum on the back side of the probe.

Table 2. Tapping Mode Tip Specification

Technical Data:		
	Value	Range
Resonant Freq.	300 kHz	+/-100 kHz
Force Constant	40 N/m	20 - 75 N/m
Length	125 μm	+/-10 μm
Mean Width	30 μm	+/-5 μm
Thickness	4 μm	+/-1 μm
Tip Height	17 μm	+/-2 μm
Tip Set Back	15 μm	+/-5 μm
Tip Radius	<10 nm	
Half Cone Angle	20°25° along cantilever axis 25°30° from side 10°at the apex	

The experiment was divided into 2 steps, dispersion of the SWNTs and XD nanotubes.

3.1 Dispersion of Nanomaterials

In each step everything was cleaned and quantitatively measured for the proper method of dispersion. The concentration of solutions was then prepared by adding 80 mL of the DMF 99% (from Acros Organic Cat#AC116220025) solvent into a 250-mL glass beaker containing 0.2 mg of nanomaterial. The solutions were then dispersed by the tip sonication technique under the hood. At 30, 60, 90 and 120 minutes, the solutions were deposited with a micropipette onto a mica substrate without filter or centrifugation, and observed by OM and AFM.

Mica substrates were obtained from Ted Pella Inc. (product# 50, quality grade V1, 9.9 mm. diameter, interleaved). To maintain a clean surface, the substrate layer was peeled with sticky tape just before the sample was deposited. After the samples were deposited, the samples were then dried over a 24 hour period. Once the 24 hour period was complete, we could observe the samples using the optical microscope. After the OM images were acquired, we moved on to analyzing the samples via the AFM. The AFM images were taken and reviewed; for additional detail, a section analysis of the first and last images was obtained.

4.0 RESULTS AND DISCUSSION

Each step of the dispersion method for the SWNT and XD nanotubes was carried out prior to performing OM and AFM. The following section provides the experimental results obtained from the procedures, briefly summarized again, below.

4.1 Dispersion of SWNTs

A tip sonicator was used in the dispersion method of CNTs. Prior to beginning the experiment, glass beakers were carefully washed and cleaned with acetone. The SWNT nanomaterial (0.2 mg) was then weighed onto weigh paper using a digital analytical balance, and placed into a glass beaker. Next, 80 mL of DMF were measured using a manual pipette and then added to the glass beaker with the SWNT nanomaterial. The solution and nanomaterial mixture were then placed within a fume hood so the odor would be greatly reduced. The tip sonication was also placed under the hood for the dispersion process. The tip sonicator was programmed for different time intervals, namely 30, 60, 90 and 120 minutes. When each sonicator time ended, a micropipette was used to remove a drop of the dispersion and place it upon a mica substrate. The sample of mica substrate was then placed onto another mica substrate layer peeled with sticky tape; the new clean layer was investigated with OM and AFM, shown as Figure 8 and Figure 9, respectively. Figure 8 shows the clean surface of the mica. The mica was transparent with a light brown color. The non-focus features on the image indicate the double side tape that lies under the mica. The focused line across the image indicates an edge of the mica layer. The clean and flat surface of the mica was confirmed with the AFM image shown as Figure 9.

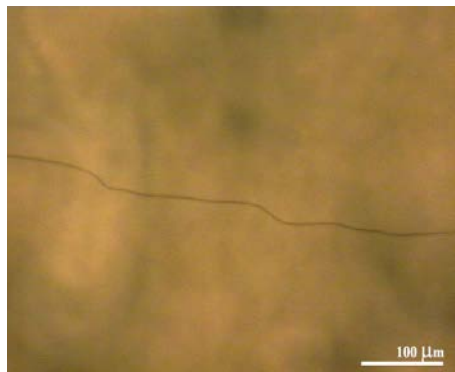


Figure 8. OM on Mica Surface

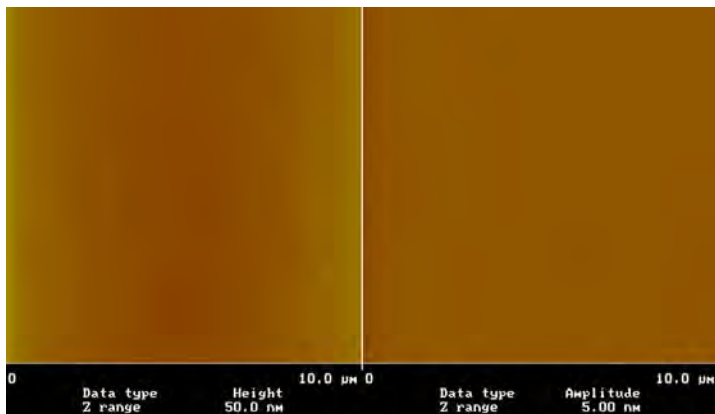


Figure 9. AFM on Mica Surface

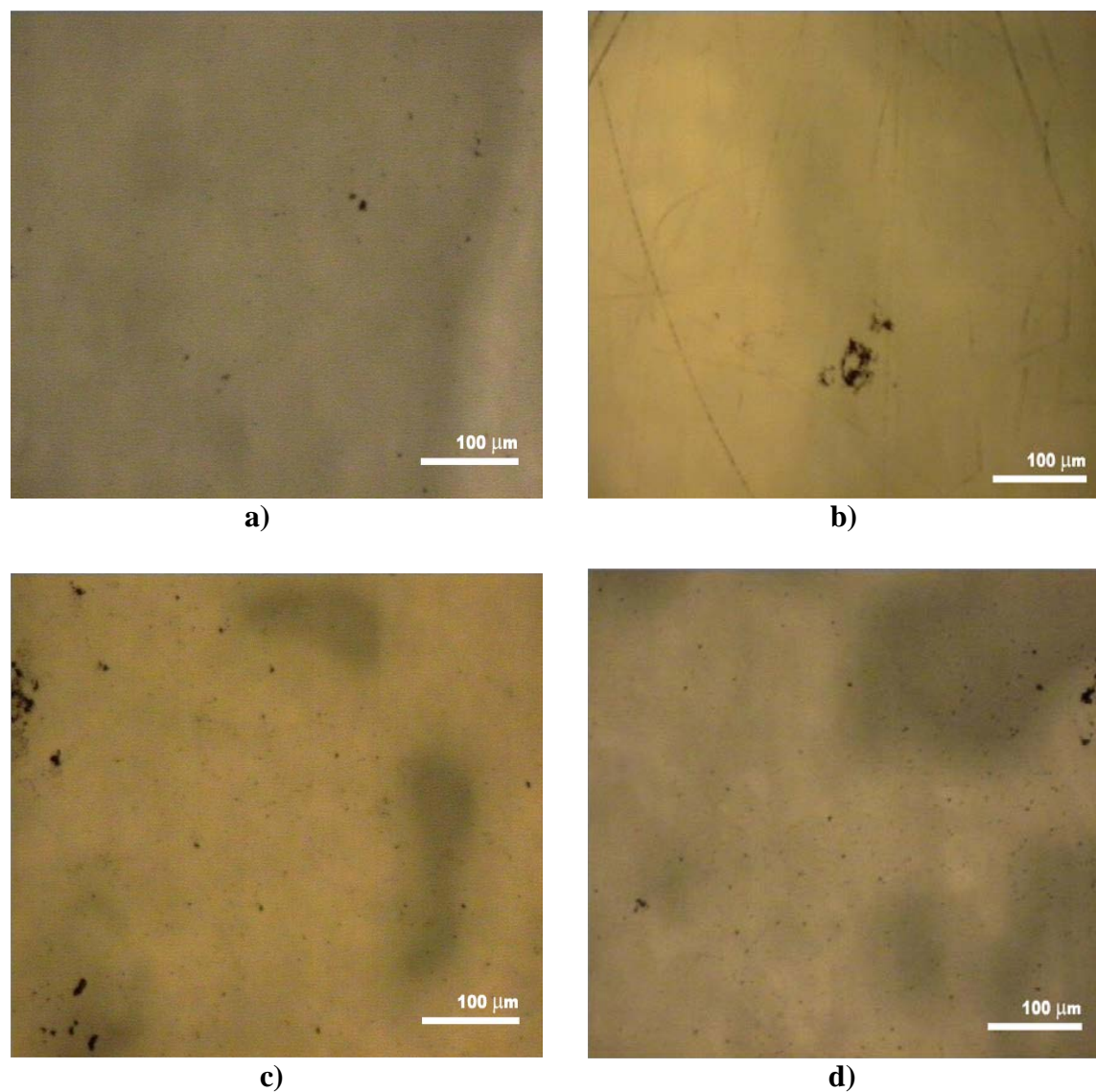


Figure 10. OM Images of SWNTs on Mica After a) 30 Minutes; b) 60 Minutes; c) 90 Minutes; d) 120 Minutes, Respectively

4.2 Ball Milling and Dispersion of XD Carbon Nanotubes (XDCNTs) and Tungsten Carbide (WC)

Mixtures of XDCNTs and WC were milled with a high-energy Spex 8000 ball milling system. The samples were removed after milling for 20, 40, 100, 160 minutes. The samples were then put in DMF at the concentration of .0025 mg/ml and tip-sonicated for 40 mins. One drop of the XDCNTs/WC/DMF solution was placed on mica and heated on a hot plate at 150°C to remove DMF. The dispersion of XDCNTs/WC nanomaterial upon mica was initially viewed with OM. Figure 10 shows those images.

An AFM image of XDCNTs/WC, after ball milling for 20 minutes and tip-sonication for 40 minutes, is shown as Figure 11. Figure 11 shows that the XDCNTs/WC was dispersed with many particles on the tubes. We were unable to tell, however, which particles were WC or

catalysts that were used during the CNTs processing. Also, parts of CNTs were still in bundles, as shown in the bottom left of Figure 12 (amplitude image).

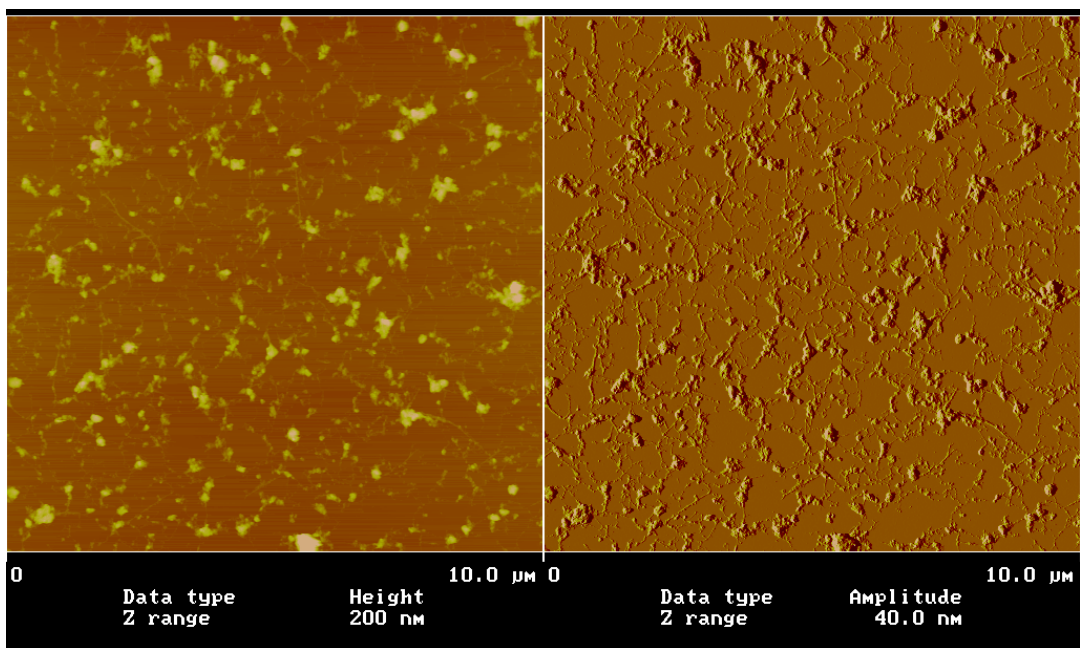


Figure 11. AFM Image of XDCNTs/WC After Ball Milling for 20 Minutes (Scan Size 10 μm)

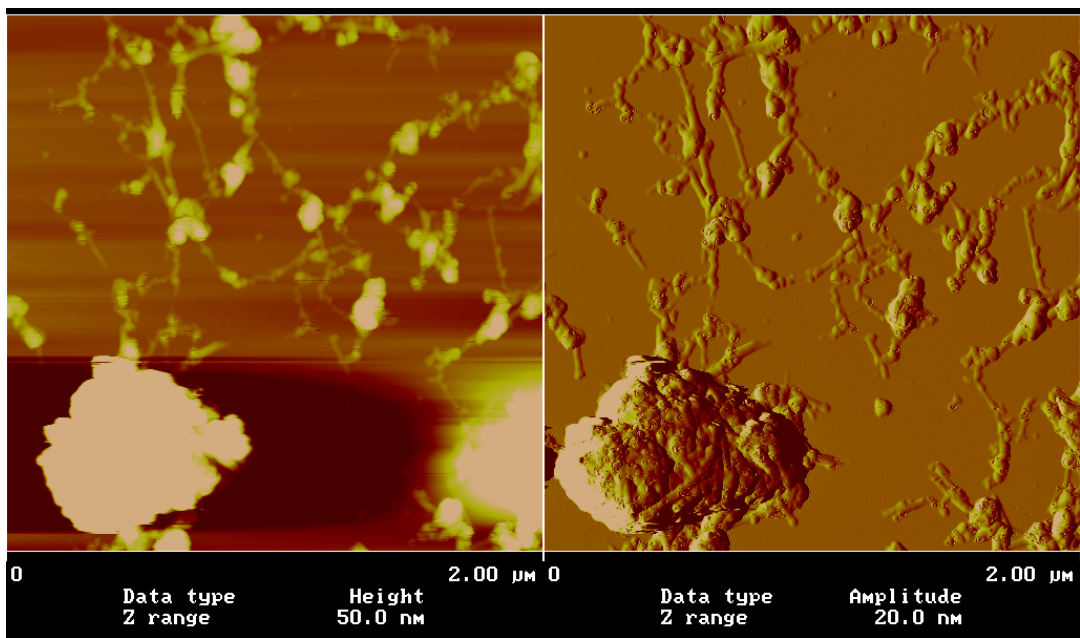


Figure 12. AFM Image of XDCNTs/WC After Ball Milling for 20 Minutes (Scan Size 2 μm)

Figure 13 and Figure 14 show AFM images of XDCNTs/WC after ball milling for 40 minutes. In comparison with Figure 11, Figure 13 shows better dispersion. This may indicate that the milling process contributes in the dispersion process. If the hypothesis is that shortened CNTs might be easier to disperse, it was not clear from Figure 11 to Figure 14 that extending the milling process from 20 to 40 minutes would shorten the nanotubes. Section analysis from Figure 14 showed that the size of the clean tubes range from 1 to 7 nm.

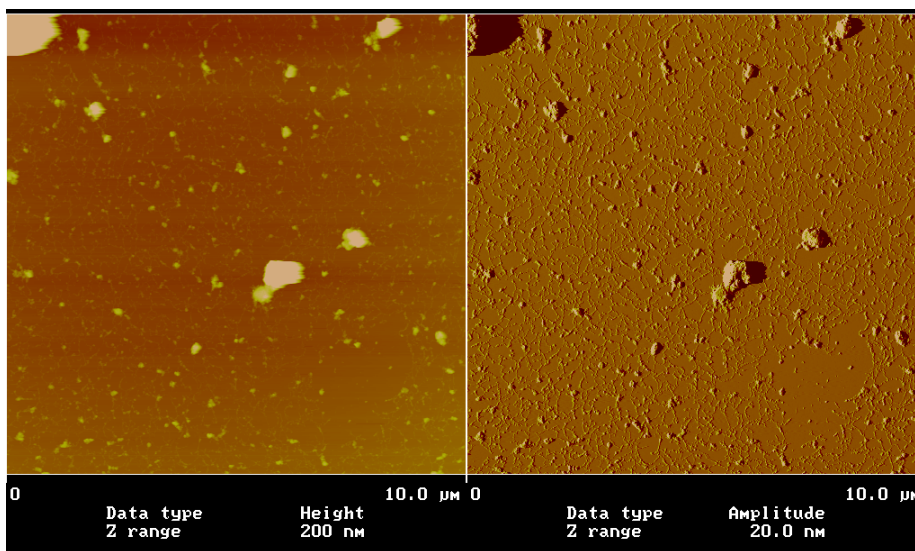


Figure 13. AFM Image of XDCNTs/WC After Ball Milling for 40 Minutes (Scan Size 10 μm)

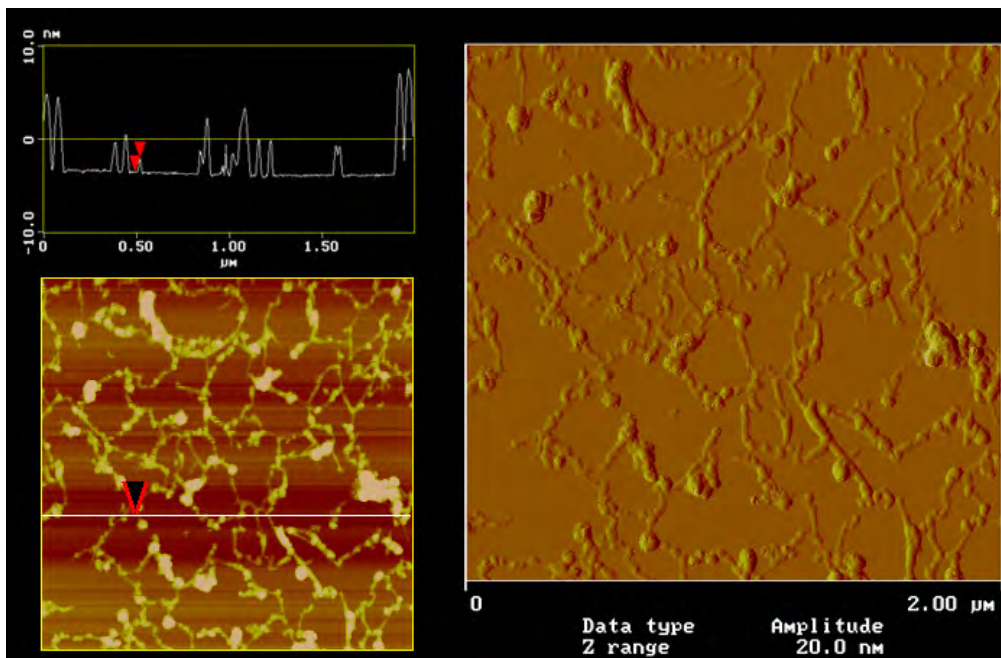


Figure 14. AFM Image and Section Analysis of XDCNTs/WC After Ball Milling for 40 Minutes (Scan Size 2 μm)

The XDCNTs/WC sample ball milling for 100 minutes was in an alcohol medium and then dried in air on aluminum foil before transfer into DMF for sonication. Figure 15 shows the AFM results after the XDCNTs/WC were tip-sonicated for 40 minutes. They appear to have large bundles along with short grain-like features all over the surface. These features could be the XDCNTs that had been shortened by the increased time on the ball milling process. Section analysis showed that the size (height) of the tubes was about 0.8 to 0.9 nm, which is about the size of typical SWCNTs. The length measurement of the tubes, shown in Figure 16, indicates that the tubes aligned in two different directions. One possible hypothesis for this occurrence is that one nanotube direction was caused from movement of the solution during drying on a hot plate, while the other direction was caused by the magnet within the hot plate.

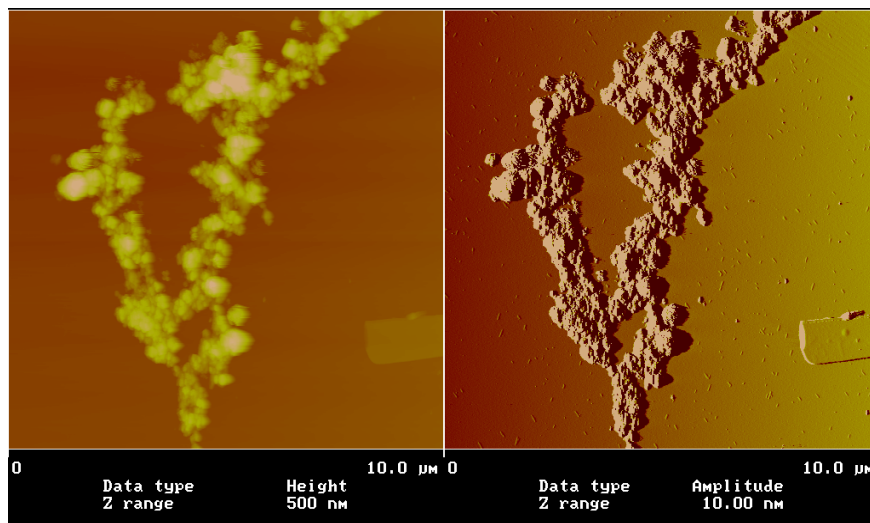


Figure 15. AFM Image of XDCNTs/WC After Ball Milling for 100 Minutes (Scan Size 10 μm)

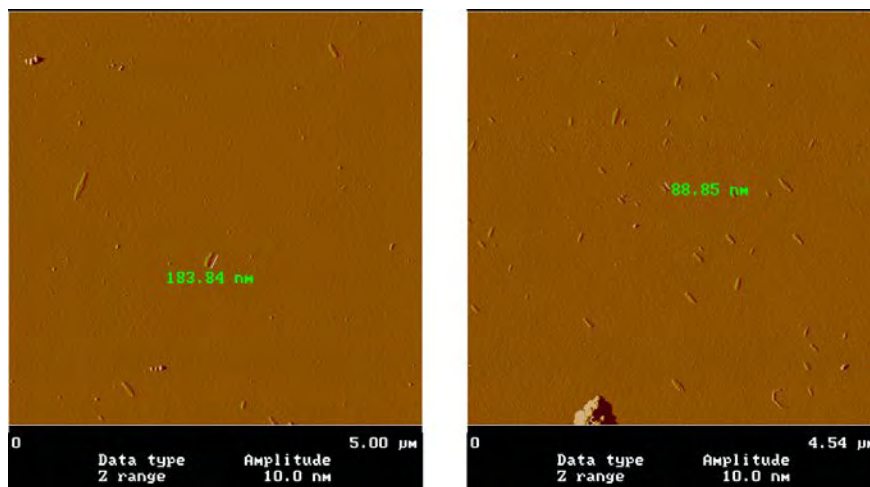


Figure 16. AFM Image and Length Measurement of XDCNTs/WC After Ball Milling for 100 Minutes

The AFM image of XDCNTs/WC after ball milling for 160 minutes is shown in Figure 17. Long cylindrical features similar to nanotubes were not noticeable. The nanotubes might have been shortened during the increased time on the ball milling process.

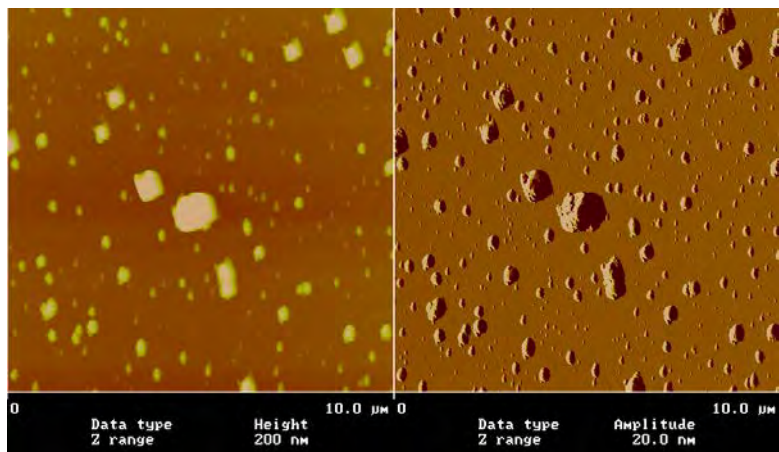


Figure 17. AFM Image of XDCNTs/WC After Ball Milling for 160 Minutes

5. CONCLUSION

The characterization of the nanomaterial was studied by using AFM, OM and section analysis.

The following conclusions were drawn:

- Of the solvents used in this research work, DMF showed promising capability as the only medium that could distribute carbon nanotubes into the fully dispersed state.
- The dispersion level of the carbon nanotubes could be roughly indicated by the OM, without the assistance of the AFM scanning mode. This can provide a quick and easier way for practical applications.
- By using the section analysis, one can distinguish between the SWNTs, DWNTs and MWNTs shown in the AFM images.
- Based upon the OM and AFM images acquired, additional investigative studies will be required in order to obtain full dispersment from both nanomaterials.

The material was provided by Clarkson Aerospace for the work on imaging. Additional samples containing different volume fractions of nanomaterials prepared by Clarkson Aerospace will be examined for future studies involving the detailed analysis of nanocomposite powders.

6. REFERENCES

1. Iijima S. *Nature* 1991;354:603e5.
2. Schadler LS, Giannaris SC, Ajayan PM. *Appl Phys Lett* 1998;73:3842e4.
3. Stephan C, Nguyen TP, Lahr B, Blau W, Lefrant S, Chauvet OJ. *Mater Res* 2002;17:396e400.
4. Dalton AB, Collins S, Munoz E, Razal JM, Ebron VH, Ferraris JP, et al. *Nature* 2003;423:703.
5. Barrau S, Demont P, Peigney A, Laurent C, Lacabanne C. *Macromolecules* 2003;36:5187e94.
6. Thostenson ET, Chou T-W. *J Phys D Appl Phys* 2003;36:573e82.
7. Coleman JN, Khan U, Blau WJ, Gun'ko YK. *Carbon* 2006;44: 1624e52.
8. Moniruzzaman M, Winey KI. *Macromolecules* 2006;39:5194e205.
9. Mitchell CA, Bahr JL, Arepalli S, Tour JM, Krishnamoorti R. *Macromolecules* 2002;35:8825e30.
10. Ramanathan T, Liu H, Brinson LC. *J Polym Sci Part B Polym Phys* 2005;43:2269e79.
11. Vaisman L, Marom G, Wagner HD. *Adv Funct Mater* 2006;16: 357e63.
12. Schaefer DW, Zhao J, Brown JM, Anderson DP, Tomlin DW. *Chem Phys Lett* 2003;375:369e75.
13. Du F, Scogna RC, Zhou W, Brand S, Fischer JF, Winey KI. *Macromolecules* 2004;37:9048e55.
14. Liao Y-H, Marietta-Tondin O, Liang Z, Zhang C, Wang B. *Mater Sci Eng A* 2004;385:175e81.
15. Song W, Windle AH. *Macromolecules* 2005;38:6181e8.
16. Song YS, Youn JR. *Carbon* 2005;43:1378e85.
17. Park C, Ounaies Z, Watson KA, Crooks RE, Smith J Jr, Lowther SE, et al. *Chem Phys Lett* 2002;364:303e8.
18. Park SJ, Cho MS, Lim ST, Choi HJ, Jhon MS. *Macromol Rapid Commun* 2003;24:1070e3.
19. Martin CA, Sandler JKW, Shaffer MSP, Schwarz MK, Bauhofer W,
20. Schulte K, et al. *Compos Sci Technol* 2004;64:2309e16.
21. Huang YY, Ahir SV, Terentjev EM. *Phys Rev B* 2006;73:125422.
22. Sennett M, Welsh E, Wright JB, Li WZ, Wen JG, Ren ZF. *Appl Phys A* 2003;76:111e3.
23. Kashiwagi T, Grulke E, Hilding J, Groth K, Harris R, Butler K, et al. *Polymer* 2004;45:4227e39.
24. Krishnamoorti R. *MRS Bull* 2007;32:341e7.
25. Balazs AC, Emrick T, Russell TP. *Science* 2006;314:1107e10.
26. L. X. Zheng et al. (2004). "Ultralong Single-Wall Carbon Nanotubes". *Nature Materials* 3: 673–676. doi:10.1038/nmat1216.
27. Mintmire, J.W.; B.I. Dunlap, and C.T. White (3 February 1992). "Are Fullerene Tubules Metallic?". *Physical Review Letters* 68: 631–634. doi:10.1103/PhysRevLett.68.631. http://prola.aps.org/pdf/PRL/v68/i5/p631_1.
28. Dekker, Cees (May 1999). "Carbon nanotubes as molecular quantum wires" (PDF). *Physics Today* 52 (5): 22–28. doi:10.1063/1.882658. <http://www.physicstoday.org/vol-56/iss-2/pdf/vol52no5p22-28.pdf>.

29. Martel, R.; V. Derycke, C. Lavoie, J. Appenzeller, K. K. Chan, J. Tersoff, and Ph. Avouris (December 2001). "Ambipolar Electrical Transport in Semiconducting Single-Wall Carbon Nanotubes". *Physical Review Letters* 87 (25): 256805. doi:10.1103/PhysRevLett.87.256805. <http://prola.aps.org/abstract/PRL/v87/i25/e256805>.
30. a b c d e Collins, Philip G.; Phaedon Avouris (December 2000). "Nanotubes for Electronics" (PDF). *Scientific American*: 67, 68, and 69. http://www.crhc.uiuc.edu/ece497nc/fall01/papers/NTs_SciAm_2000.pdf.
31. "Carbon Solutions, Inc.". <http://www.carbonsolution.com>.
32. "CarboLex". <http://carbolex.com>.
33. R. S. Ruoff, et al., "Radial deformation of carbon nanotubes by van der Waals forces" *Nature* 364, 514 (1993)
34. I. Palaci, et al. "Radial Elasticity of Multiwalled Carbon Nanotubes" *Phys. Rev. Lett.* 94, 175502 (2005)
35. M.-F. Yu, et al. "Investigation of the Radial Deformability of Individual Carbon Nanotubes under Controlled Indentation Force" *Phys. Rev. Lett.* 85, 1456-1459 (2000)
36. Ajram, K. (1992). *The miracle of Islamic science*. Knowledge House Publishers. pp. Appendix B. ISBN 0-911119-43-4.
37. Timeline - History of Microscopes
38. Microscopes: Time Line
39. Stephen Jay Gould(2000). *The Lying Stones of Marrakech*, ch.2 "The Sharp-Eyed Lynx, Outfoxed by Nature". London: Jonathon Cape. ISBN 0224050443
40. Morita, Seizo. *Roadmap of Scanning Probe Microscopy*. 3 January 2007
41. Jie Liu, Michael J. Casavant, Michael Cox, D.A. Walters, P. Boul, Wei Lu, A.J. Rimberg, K.A. Smith, Daniel T. Colbert, Richard E. Smalley, "Controlled deposition of individual single-walled carbon nanotubes on chemically functionalized templates", *Chemical Physics Letters* 303 (1999),125–129.
42. Kevin D. Ausman, Richard Piner, Oleg Lourie, and Rodney S. Ruoff, "Organic solvent dispersions of single-walled carbon nanotubes: Toward solutions of pristine nanotubes", *J. Phys. Chem. B*, Vol. 104, No. 38, 2000
43. Bumsu Kima, Yun-Ho Lee, Jee-Hyun Ryu, Kyung-Do Suh, "Enhanced colloidal properties of single-wall carbon nanotubes in α -terpineol and Texanol", *Colloids and Surfaces A: Physicochem. Eng. Aspects* 273 (2006) 161–164.
44. Yi Lin, Shelby Taylor, Huaping Li, K. A. Shiral Fernando, Liangwei Qu, Wei Wang, Lingrong Gu, Bing Zhou and Ya-Ping Sun, "Advances toward bioapplications of carbon nanotubes", *J. Mater. Chem.* ,2004, 14, 527–541
45. M. F. Islam, E. Rojas, D. M. Bergey, A. T. Johnson, and A. G. Yodh, "High weight fraction surfactant solubilization of single-wall carbon nanotubes in water", *Nano Lett.*, Vol. 3, No. 2, 2003, 269-273.
46. Michael S. Strano, Valerie C. Moore, Michael K. Miller, Mathew J. Allen, Erik H. Haroz, Carter Kittrell, Robert H. Hauge, and R.E. Smalley, "The role of surfactant adsorption during ultrasonication in the dispersion of single-walled carbon nanotubes", *J. Nanosci. Nanotech.*, 2003, Vol. 3, No.1/2, 81-86.
47. Rajdip Bandyopadhyaya, Einat Nativ-Roth, Oren Regev, and Rachel Yerushalmi-Rozen, "Stabilization of individual carbon nanotubes in aqueous solutions", *Nano Lett.*, Vol. 2, No. 1, 2002, 25-28.

48. Hyeong Taek Ham, Yeong Suk Choi , In Jae Chung, “An explanation of dispersion states of single-walled carbon nanotubes in solvents and aqueous surfactant solutions using solubility parameters”, *Journal of Colloid and Interface Science* 286 (2005) 216–223.
49. Jeffrey A. Fagan, Matthew L. Becker, Jaehun Chun, and Erik K. Hobbie, “Length fractionation of carbon nanotubes using centrifugation”, *Adv. Mater.* 2008, 20, 1609–1613.
50. Michael S. Arnold, Alexander A. Green, James F. Hulvat, Samuel I. Stupp, Mark C. Hersam, “Sorting carbon nanotubes by electronic structure using density differentiation”, *Nature Nanotechnology*, Vol 1, October 2006, 60-65.

7. LIST OF SYMBOLS, ABBREVIATIONS AND ACRONYMS

A	Ampere
Å	Ångstrom
AFM	Atomic Force Microscope
CCD	Charge-Coupled Device
CCVD	Combustion Chemical Vapor Deposition
CNT	Carbon Nanotube
cP	Centipoise
CVD	Chemical Vapor Deposition
DMF	<i>N,N</i> -Dimethylformamide
DMSO	Dimethyl sulfoxide
DWNT	Double-Walled Carbon Nanotube
FET	Field Effect Transistor
GPa	Gigapascal
IPA	Isopropyl Alcohol
kg/m ³	Kilogram per cubic meter
KHz	Kilohertz
MFM	Magnetic Force Microscope
mg/ml	Milligram per milliliter
MWCT	Multi-Walled Carbon Nanotube
N/m	Newton per meter
nm	Nanometer
NMP	N-methylpyrrolidone
OLED	Organic Light Emitting Diode
OM	Optical Microscope
pl	Pico Liter
RFC	Relative Centrifugal Forces
rpm	Round Per Minute
S/cm	Siemen Per Centimeter
SC	sodium chlorate
SCM	Scanning Electron Microscope
SDBS	sodium dodecylbenzenesulfonate
SDS	sodium dodecyl sulfate
SFM	Scanning Force Microscope
SPM	Scanning Probe Microscope
STM	Scanning Tunneling Microscope
SWNT	Single-Walled Carbon Nanotube
TCA	1,1,1-Trichloroethane
TEM	Transition Electron Microscopy
TPa	Terapascal
V	Volt
W	Watt
w/w	Weight by Weight
WC	Tungsten Carbide
XDCNT	XD Carbon Nanotube

μm	Micrometer
$\mu\text{m/s}$	Micrometer per second
$^{\circ}\text{C}$	Degree Celsius
-cm	Ohm-centimeter